A Study on a Digital Twin of Electrified Railway Systems

In Kwon Park†[1], Sachintha Kariyawasam[2], Dean Ouellette[3], Yi Zhang[4]
Joorak Kim[5], Gyu-Jung Cho[6]

Abstract – As the effort to reduce the carbon footprint of transportation becomes more intensified, significantly more attentions are turning towards electrified railway systems. Electrified railway systems have been more efficient in the utilization of the energy resources and inherently less carbon oriented in the way of driving the outcome from the energy input. Long before the road-centric mode of transportation such as trucks and cars turned to electrification, the railway system began turning to electricity as the prime source of energy. Consequently, certain countries already electrified more than 70% of their railway systems. Another outstanding characteristic of the electrified railway system is its closer integration to the energy system with the control and monitoring system. The interactions due to this tight integration require detailed studies with precise modelling and simulation. Through the modelling and simulation, the system designers, as well as the operators, can get a more precise understanding regarding the planning and operation of an electrified railway system. In this paper, a digital twin of an electrified railway system is introduced. The proposed digital twin includes a feeder transformer, its detailed protection system models, and a train model as a moving load in the supply system. The impact of such characteristics upon the protection system are investigated in detail and the results are presented.

Keywords: Electrified Railway System; Modelling; Simulation

1. Introduction

Since Siemens was able to demonstrate the possibility of driving a train by electricity in 1879[1], Electrification of railway systems has been making progress. In recent years, the progress came under a new light of attention. The awareness of the climate change and the concerns for carbon emission, is increasing. Many governments are taking various ways to deter the uncontrolled growth of carbon-centric energy consumption. One such measure is the ban of internal combustion engine cars. Similarily, the railway industry is seeking for higher level of electrification. Meanwhile, such progress is not exclusively observed in urban settings such as metro style mode of transportation, where the combustion exhaust would create more serious issues, including the residents' complaints.

The ever-increasing demand for the higher speed of travel and shorter travel time, both for passengers and freights, is pushing the need for the electrification to a new level. One such example is the Linear Chuo Shinkansen in Japan[2]. Current trial runs at the Yamanashi testing center/track move the test L0 series train around 500km/h. However, the target speed of the project and its operator (JR-Dokai) is to be around 800km/h, eventually. Such a high speed is in the same range as that of commercial airliners. However, the ability of the transportation in the same amount of time (e.g., the number of passengers per hour) and the level of comfort (e.g., accessibility to the metro area) is far superior to the service by airliners. While the speed of the new transportation is certainly impressive, the energy consumption of the mode of transportation is also comparable to that of a commercial airliner. Per seat/per distance energy consumption of the new Linear Chuo Shinkansen is about 90-100Wh/seat/km[3], which would be close to 80% of the per seat/per distance energy consumption of a commercial aircraft (e.g., Boeing 737). Subsequently, the entire train system would put the energy supply system, i.e., the railway feeder system and its associated transmission system, into an unprecedented level of stress. While the amount of the energy supply poses its own set of issues, the quality of the supply would also create a new set of problems. The magnetic levitation, both in the vertical axis (levitation in the usual sense) as well as the horizontal axis (a train guide + propulsion) must be strictly maintained. In the case of the Linear Chuo Shinkansen, a series of super conducting magnets on the wall of the train guide as well as the side wall of the train takes charge of maintaining the necessary magnetic field. In an expected

1,† Corresponding Author: RTDS Technologies Inc., Winnipeg, Canada (parkik@rtds.com)
2: RTDS Technologies Inc., Winnipeg, Canada (sachintha@rtds.com)
3: RTDS Technologies Inc., Winnipeg, Canada (dean@rtds.com)
4: RTDS Technologies Inc., Winnipeg, Canada (yzhang@rtds.com)
5: Korea Railroad Research Institute, Korea (jrkim@krri.re.kr)
6: Korea Railroad Research Institute, Korea (gjcho@krri.re.kr)

operation scenario, a single set of train would run in excess of 600km/h speed and the total weight of the train set would be the upper side of 500 metric ton (each coach car would weigh about 25 ton with no passenger). During its full speed run, the leeway the system would allow in terms of the levitation gap becomes very small. Therefore, high precision is designed and expected in every single part of the entire traction system, including the energy supply system. Such tight margin requirement is not confined to the train itself. The levitation is achieved by super conducting magnets. The magnets are to be kept in the super conduction state by cryogenic systems. Simply speaking, the cryogenic system is an enlarged version of a refrigerator. The cryogenic system cools the working fluid in the same way as a refrigerator freezes water to make ice. However, in the cryogenic system the working fluid is liquid helium at extremely low temperature, -269C or 4.22 K. Therefore, the failure of the cryogenic system would cause the quench of the super conducting coil in the magnets. The loss of subsequent levitation and traction, where the super conducting magnets are holding the critical roles, would follow. Eventually, the consequence of the quench (i.e., loss of super conducting state) would lead to an accident in the system, resulting in catastrophic consequence.

This paper presents a way to address the need to the test and evaluate of an electrified railway system. The focus of the proposed idea is to establish a digital twin of an electrified railway system, by utilizing real-time modelling and simulation of traction systems. The on-board traction systems are run by the combination of a motor drive system and a traction motor. After the introduction, the paper presents real-time simulation models addressing the individual components of the electrified railway system. The usefulness of the approach is presented by a realistic real-time simulation case, where a protection system of the feeder transformer (Scott transformer) is evaluated with a train moving in pre-defined schedule. The paper finishes with a set of concluding remarks.

2. MODELLING OF ELECTRIFIED RAILWAY SYSTEM COMPONENTS

In order to build a digital twin of an electrified railway system, all the necessary devices in a real system which the digital twin attempts to mimic need to be modelled in mathematical way. In other words, each individual device should be described in the mathematical expression in the necessary level. Often, the expressions are made up by the combination of a set of differential equations and algebraic equations (DAEs). An ideal way to solve the expression would be through an analytical way. However, in practice, solving a set of differential equations would found to be difficult, if not impossible, within given restrictions. The restrictions would include the extent of expressions (e.g., the limit of the numerical precision) as well as the allowed amount of time to solve. For example, if solving a set of differential equation would take a month, then such solution would be meaningful in a theory, but becomes useless in any practical application of the digital twin. Therefore, instead of utilizing an analytical solution to come up with the solutions, a numerical integration technique is utilized and the set of the DAEs are solved in the time domain. Such an approach is usually referred to as time domain simulation. This way of simulation has been widely accepted to depict a real-world system. Many software packages which would accomplish such numerical time domain simulations are addressing the need of the digital twin. While, those softwares would address a certain level of needs, more stringent requirement comes with the real time requirement[4]. For example, a user would plan to test a real world device, e.g., a controller of an on-board 4-Q converter system, such plan would assume that the controller would interact with a real-world system in the same way in a simulated digital twin. In other words, the numerical time domain simulation should run in the strict synchronism with the real-world clock. Simply speaking, one second in the world of digital twin should be exactly one second in the real world. Such stringent requirement would draw a clear line between non real-time, time-domain simulation software and real-time, time-domain simulation software/hardware. Furthermore, such requirement would exclude many simulation techniques, which, would enhance the accuracy of the time domain simulation, with the price of a longer execution time. One such technique is interpolation. In digital time domain simulation, the time step determines when any external stimulus to the simulation is sampled and the corresponding reaction of the rest of system is calculated. Simply speaking the time step is analogous to the time step given to the process of A/D conversion. The quantization error of a certain A/D conversion is not only from the limited resolution of the A/D converter, but the size of time step also contributes to the error. In order to overcome the limit given by the size of time step, many off-line simulation software are attempting what is usually referred to as interpolation. Two such examples are presented here: one is from a widely used EMTP[5] type power system simulation software, PSCAD and the other is from another widely used power electronics simulation software, PSIM. In the case of PSCAD, the way how the interpolation is explained in [6]. Simply speaking, the software would be able to capture the exact timing of a transition, usually referred to as zero crossing, then the simulation execution algorithm moves back to the exact moment. Then, the algorithm, proceed to one regular time step, then it moves back the simulation results to the original time step boundary. The detailed

process of the interpolation is given in the following figure, Figure 1:

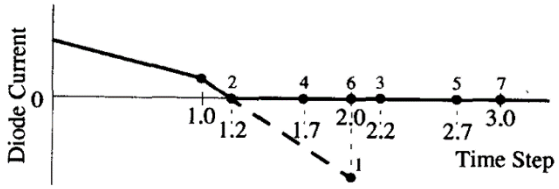

Figure 1 Interpolation in PSCAD[6]

In the figure, Figure 1, the integer indexes appearing over the time step axis shows the number of sequence of events, while those floating-point number appearing under the same axis present the portion of the time step. One point to notice is that throughout the process, the integration method remains the same. In other words, the trapezoidal rule carries all the necessary numerical integrations through the interpolation process.

In the case of PSIM, a different version of the interpolation comes into the simulation whenever the simulation engine detects the event of zero crossing. The technique is well explained in [7]. Simply speaking, when the simulation engine detects an event which would satisfy the pre-defined criteria, the simulation engine would go back 1 regular time step, then it divides the time step into two equal length sub time steps, then it changes the integration method from the regular trapezoidal method to a simpler backward Eular (BE) method.

Both methods assume the free use of the time step. In other words, both methods go back and forth in the time axis as necessary. Such free use of the time in the simulation time axis is only possible in the non-real time simulation. Once the simulation requirement of the digital twin requires real time, then such freedom disappears. In other words, the past is the past in real time simulation. There is no way to go back to the past, the same as in real world, Therefore, the modelling and the numerical representation of a device in the simulation would take in an additional requirement, the real time running. While the aforementioned interpolation technique would impose extra requirement regarding writing the numerical representation of a device, the real time restriction on the real time simulation would come with its own rules regarding how to write a numerical model. Therefore, the models in the digital twin need to ensure that they will follow such a new requirement. In the electrified railway system digital twin, presented in this paper, there are a series of devices which would carry a certain level of importance in terms of making the digital twin match its real-world counterpart. These devices include, a 3-phase to 2-phase transformer (Scott Transformer) and its protection system, the train and its propulsion system. Each of those devices are described in a brief manner in the following sections.

2.1 A train and its propulsion system

The digital twin presented in this paper assumes a metro style electrified train. The metro style trains are different from high-speed passenger trains. The highest train speed is restricted by the urban settings, which would raise particular concerns regarding the noise and vibration. Then, the distance between the stations becomes much shorter, often it becomes less than a kilometer. Whereas, in the case of high-speed passenger train, the maximum speed is limited by its own design, therefore the speed can go up to the upper side of 300km/h. Then, the distance between the stations in the case of high-speed passenger train becomes much longer, usually in the range of 50~200km between major population centers. Consequently, the design objectives of those two types of trains becomes different.

The usual choice of the main propulsion system in a metro style electrified train is to use squirrel cage type induction motors. The rotor of the machine is a squirrel cage, a simple structure with no electrical connection to the outside. Moreover, the rotor and the stator of the machine does not impose a strict requirement in terms of cooling. Therefore, a simpler cooling system such as natural air flow would become sufficient. Therefore, the usual design choice is putting the machine into a bogie with its speed reduction gear. The following figure, Figure 2, shows a typical configuration of a propulsion drive system.

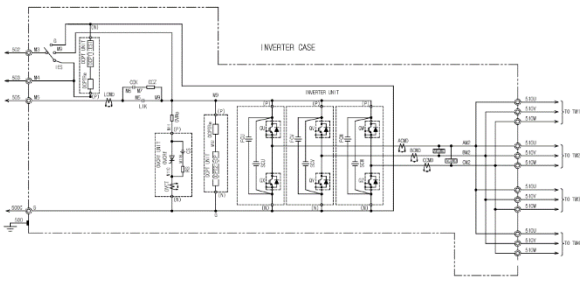

Figure 2 A VVVF main circuit[8]

The Variable Voltage Variable Frequency (VVVF) drive system can be made small enough to fit into the narrow space between underneath the train car floor and the rail. One added benefit of the compactness of the propulsion system is that a traction car can constructed in a self-contained manner. In other words, all the necessary systems such as the propulsion system, a main transformer, a 4-Q converter and so on can be put under the floor of a single car. Such self-contained car offers the freedom of pick and choose when a train set is composed. Furthermore, when the system

operator, e.g., metro line operator in a city, needs to store the necessary amount of the cars as a reserve, such self-contained car would offer the flexibility in terms of the types of the cars to be stored in the reserve.

The following set of equations defines the squirrel induction machine in a DQ domain[9]:

Stator side:

$$V_{ds}^{\omega} = \mathrm{R}_s i_{ds}^{\omega} + \frac{d(\lambda_{ds}^{\omega})}{dt} - \omega\lambda_{qs}^{\omega} \quad (1)$$

$$V_{qs}^{\omega} = \mathrm{R}_s i_{qs}^{\omega} + \frac{d(\lambda_{qs}^{\omega})}{dt} + \omega\lambda_{ds}^{\omega} \quad (2)$$

$$V_{ns}^{\omega} = \mathrm{R}_s i_{ns}^{\omega} + \frac{d(\lambda_{ns}^{\omega})}{dt} \quad (3)$$

Rotor side:

$$V_{dr}^{\omega} = \mathrm{R}_r i_{dr}^{\omega} + \frac{d(\lambda_{dr}^{\omega})}{dt} - (\omega - \omega_r)\lambda_{qr}^{\omega} \quad (4)$$

$$V_{qr}^{\omega} = \mathrm{R}_r i_{qr}^{\omega} + \frac{d(\lambda_{qr}^{\omega})}{dt} + (\omega - \omega_r)\lambda_{dr}^{\omega} \quad (5)$$

$$V_{nr}^{\omega} = \mathrm{R}_r i_{nr}^{\omega} + \frac{d(\lambda_{nr}^{\omega})}{dt} \quad (6)$$

The transformation matrix, which defines the transformation from phase domain to the DQ domain is given by the following expression:

$$\mathrm{T}(\theta) = \frac{2}{3}\begin{bmatrix} \cos(\theta) & \cos(\theta - \frac{2}{3}\pi) & \cos(\theta + \frac{2}{3}\pi) \\ -\sin(\theta) & -\sin(\theta - \frac{2}{3}\pi) & -\sin(\theta + \frac{2}{3}\pi) \\ \frac{1}{\sqrt{2}} & \frac{1}{\sqrt{2}} & \frac{1}{\sqrt{2}} \end{bmatrix} \quad (7)$$

The usual choice of the VVVF control is FOC (Field Oriented Control). There are many different techniques to achieve the given purpose, the control of the propulsion machine under the category of the FOC. Those techniques can be categorized into two subcategories. One is direct FOC and the other is indirect FOC. The criterion which marks the border between these two categories is whether there is an explicit way of measuring the speed of the machine, for example by an encoder. The traction system comes with higher level of concern for the safety than a usual consumer-oriented product with a drive system such as a washing machine. Therefore, there is less motivation of taking out part of the system components for the sake of the cost reduction. Consequently, most of the traction systems are equipped with the necessary speed measurement system. Often, such systems comes with the level redundancy determined by the safety requirement to ensure the safe operation of a train. As a result, the speed information of a machine is usually readily available, making the indirect-FOC as a good choice of the VVVF control algorithm. The algorithm can be described as follows, in a succinct way.

Starting from Q-axis rotor voltage equation:

$$V_{qr}^{\omega} = \mathrm{R}_r i_{qr}^{\omega} + \frac{d(\lambda_{qr}^{\omega})}{dt} + (\omega - \omega_r)\lambda_{dr}^{\omega} \quad (8)$$

If the reference frame is synchronized with rotor flux rotating frame, then the equation can be written in this way:

$$V_{qr}^{e} = \mathrm{R}_r i_{qr}^{e} + \frac{d(\lambda_{qr}^{e})}{dt} + (\omega_e - \omega_r)\lambda_{dr}^{e} \quad (9)$$

If the FOC control is working well, then one can assume that $\lambda_{qr}^{e} = 0$. If the rotor of the induction machine is shorted (i.e., squirrel cage rotor), then the equation can be simplified further:

$$0 = \mathrm{R}_r i_{qr}^{e} + (\omega_e - \omega_r)\lambda_{dr}^{e} \quad (10)$$

From this equation, the slip (=ω_{sl}) can be calculated in this way:

$$(\omega_e - \omega_r) = \omega_{sl} = -\frac{\mathrm{R}_r i_{qr}^{e}}{\lambda_{dr}^{e}} \quad (11)$$

The following equation can be used to replace a rotor current value (=i_{qr}^{e}) with a stator current:

$$\lambda_{qr}^{e} = 0 = L_r i_{qr}^{e} + L_m i_{qs}^{e} \quad (12)$$

$$i_{qr}^{e} = -\frac{L_m}{L_r} i_{qs}^{e} \quad (13)$$

Once the rotor current value is replaced, the slip information necessary for flux position estimator (so called 'flux observer') can be derived by the following expression.

$$\omega_{sl} = \frac{\mathrm{R}_r L_m i_{qs}^{e}}{L_r \lambda_{dr}^{e}} \quad (14)$$

2.2 A 3-phase to 2-phase transformer (Scott Transformer)

One outstanding feature of an AC electrified railway system is that the system is operated as a single-phase system. In other words, a train would get the necessary electric power from a single line, usually an overhead catenary line, while the train wheels become the ground as they contact the rails. Frequently, the single-phase system at the railway side is supplied by a transmission level system owned by a public utility. Practically, all such transmission level systems are configured as a three-phase system. When a single-phase system is interfaced with a three-phase system, another issue comes up. It imposes the unbalanced loading on the three-phase side. Such unbalance would cause many undesirable effects at the transmission system side. One typical example is the negative sequence voltage and current. Therefore, in order to satisfy those two given conditions, 1) 3-phase to 1 or 2-phase 2) 3-phase side unbalance, many different transformer topologies were developed and utilized. Such transformer topologies include Scott, Le Blanc, Woodbridge, modified Woodbridge[10] and V connections[11]. In Korean railway systems and part of Japanese railway systems, the Scott Transformer became a standard way of interfacing the railway electrical system to a transmission level system. In theory, two single phase transformers can be connected together with certain turns ratio between their primary and secondary side for the purpose of generating 2 single-phase outputs at the secondary side. The phase angle between the first transformer output and the second transformer output come as 90-degree shift. One result of such a transformer

configuration is that when the secondary side of each of those single-phase transformers is equally loaded, the corresponding primary side would maintain the balance. Therefore, the balanced loading at the secondary side would achieve the balance at the primary side which would be desired by the operator of the transmission system. The following figure, Figure 3, presents such configuration, using two single-phase transformers.

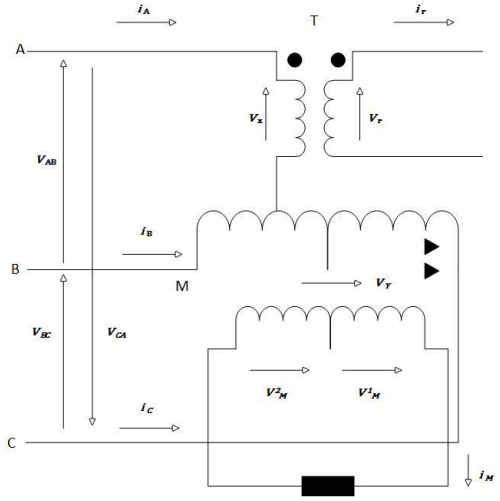

Figure 3 A Scott transformer[12]

The voltage relationship between the primary side and the secondary side are described by the following equations:

$$a = \frac{n1}{n2} \tag{15}$$

$$VT = \frac{2\sqrt{3}Vx}{3a} \tag{16}$$

$$VM = \frac{Vy}{a} \tag{17}$$

$$VAB = Vx + \frac{Vy}{2} \tag{18}$$

$$VBC = -Vy \tag{19}$$

$$VCA = \frac{Vy}{2} - Vx \tag{20}$$

The Vx and Vy can be expressed by these two equations:

$$Vx = \frac{VTa\sqrt{3}}{2} \tag{21}$$

$$Vy = VMa \tag{22}$$

Then, the primary side voltage values can be expressed by the secondary side voltage values.

$$VAB = \frac{VTa\sqrt{3}}{2} + \frac{VMa}{2} \tag{23}$$

$$VBC = -VMa \tag{24}$$

$$VCA = \frac{VMa}{2} - \frac{VTa\sqrt{3}}{2} \tag{25}$$

Consequently, a transformation matrix can be defined which depicts the relationship between the primary side voltage values and the secondary side ones.

$$\begin{bmatrix} \frac{a\sqrt{3}}{2} & \frac{a}{2} \\ 0 & -a \\ -\frac{a\sqrt{3}}{2} & \frac{a}{2} \end{bmatrix} \tag{26}$$

The current relationship between the primary side and the secondary side are described by the following equations. The direction notations can be seen in the Figure 3.

$$\frac{\sqrt{3}n1iA}{2} = n2iT \tag{27}$$

$$\frac{1}{2}n1iC - \frac{1}{2}n1iB = n2iM \tag{28}$$

Because the following relationship establishes,

$$iA + iB + iC = 0 \tag{29}$$

Another transformation matrix defining the relationship between the primary side current values and the secondary side ones can be written:

$$\begin{bmatrix} \frac{2\sqrt{3}}{3a} & 0 \\ -\frac{\sqrt{3}}{3a} & -\frac{1}{a} \\ -\frac{\sqrt{3}}{3a} & \frac{1}{a} \end{bmatrix} \tag{30}$$

2.3 A 87T Scott Transformer differential protection element

Similar to most transformers in power systems, the Scott transformers in metro train systems can be effectively protected using current differential protection schemes. Figure 4 illustrates typical CT connections for current differential protection of a Scott transformer. It is important to note that a Scott transformer has five currents in total but only two independent cores. As a result, a Scott transformer can be protected with only two independent current differential elements with special connection arrangements. In contrast, a regular 3-phase power transformer typically requires three elements, one for each phase. Shown in Figure 5 are the primary (Ia, Ib and Ic in red) and secondary (IM and IT in blue) current phasors of a Scott transformer under balanced load conditions. Note that direction of current measurements are as indicated in Figure 4 (currents flowing into the transformer are considered positive).

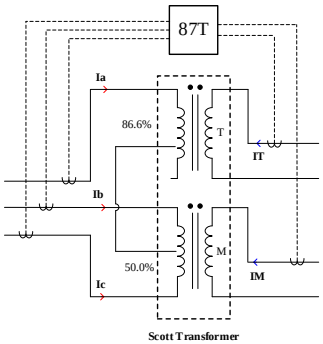

Figure 4 Scott Transformer connections for current differential protection

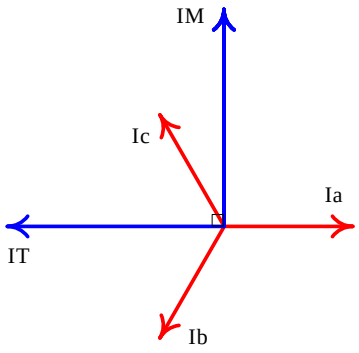

Figure 5 Primary (red) and secondary (blue) current phasors of a Scott Transformer under balanced load conditions

Applying MMF (ampere-turns) balance to each of its two independent cores, one can derive the ideal relationship between primary and secondary currents of a Scott transformer, which is given in (31) below in matrix form. V_{pri} and V_{sec} are rated primary and secondary voltages of the Scott transformer, respectively.

$$\begin{bmatrix} IT \\ IM \end{bmatrix} = \frac{V_{pri}}{V_{sec}} \begin{bmatrix} -\sqrt{3}/2 & 0 & 0 \\ 0 & -1/2 & 1/2 \end{bmatrix} \begin{bmatrix} I_a \\ I_b \\ I_c \end{bmatrix} \quad (31)$$

A dedicated current differential protection relay simulation model was developed to protect Scott transformers. This model takes all five currents of a Scott transformer as inputs and comprises of two independent two-slope current differential elements (87T). Based on (31), the operating and restraint quantities (currents) of the two current differential elements are expressed in (32) and (33) below. Note that the transformer connections are made in such a way that the phase A (primary) and the teaser (secondary) windings are connected to one core (corresponds to 87T element 1) of the Scott transformer, whereas phases B, C (primary) and the main (secondary) windings are associated with the second core (corresponds to 87T element 2).

$$\begin{aligned} I_{op\,1} &= \left| \frac{V_{pri}}{V_{sec}} . \frac{\sqrt{3}}{2} . I_a + I_T \right| \\ I_{r\,1} &= \frac{1}{2} \left\{ \left| \frac{V_{pri}}{V_{sec}} . \frac{\sqrt{3}}{2} . I_a \right| + |I_T| \right\} \end{aligned} \quad (32)$$

$$\begin{aligned} I_{op\,2} &= \left| \frac{V_{pri}}{V_{sec}} . \frac{1}{2} . (I_b - I_c) + I_M \right| \\ I_{r\,2} &= \frac{1}{2} \left\{ \left| \frac{V_{pri}}{V_{sec}} . \frac{1}{2} (I_b - I_c) \right| + |I_M| \right\} \end{aligned} \quad (33)$$

For each 87T element, the operating current (Iop) is determined by the vector sum of the respective currents. On the other hand, the restraint current (Ir) is calculated using the summation of current magnitudes divided by one-half. The relay model employs a DFT algorithm to extract the fundamental as well as the second harmonic magnitudes of the current inputs. Transformer protection elements use an additional measurement ratio of second harmonic over fundamental (current) to prevent mis-operation during transformer energization. The two-slope differential current characteristic that governs the operation of the 87T element of the relay model is given in the following figure, Figure 6.

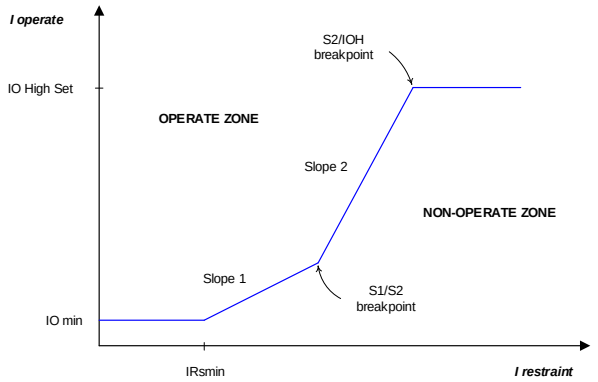

Figure 6 Two-slope differential current characteristic

The differential characteristic defines the amount of operating current required to assert the 87T element for different restraint current levels. The operating quantity must be above the minimum operating value setting (IOmin) for the 87T element to operate. If the restraint current increases above the value of IRsmin, the amount of operating current necessary to make the relay operate increases along Slope1. Likewise, if the restraint current increases beyond the Slope1/Slope2 (S1/S2) breakpoint, the amount of operating current necessary increases along Slope2, which generally has a steeper gradient than Slope1. The element asserts for all operating currents above the IOH high-set value. All the parameters necessary to define the above differential characteristic can be specified in the relay model. Once asserted, each 87T element issues a trip signal, which can be used for operating the corresponding circuit breakers in the simulation.

3. A DEMONSTRATION

A RTDS™ simulation case was constructed as a digital twin of an electrified railway system. The simulation case includes the aforementioned components, the trainset with its drive system, Scott transformers and the 87T Scott Transformer differential protection elements. The simulation case runs in real time, with the given time step size of 50uS for the regular time step portion of the simulation. The size of time step becomes much smaller than the regular time step portion, in order to capture the high frequency transients occurring at the power electronics system which comprises the traction motor drive system. The size of smaller time step is set as 5us, $1/10^{th}$ of the regular time step size. The

following figure, Figure 7, presents the outlook of the simulation case.

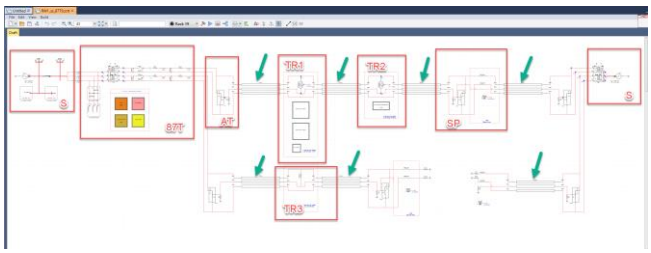

Figure 7 A RTDS railway simulation

The boxes labeled 'S' represent the utility grid network. The transmission is the energy supply to the electrified railway network, at the voltage level of 154kV. The utility transmission network is connected to a Scott transformer. The secondary side voltage level of of the transformer is 55kV[13], which is 2 times as large as the 1-phase railway feeder system voltage. The nominal voltage is 25kV, while at the secondary side of the Scott transformer, the voltage is set to a little bit higher value, at 27.5kV. The 55kV voltage from the Scott transformer secondary side is split to 2 27.5kV output by an autotransformer. The neutral of the transformer is connected to the rail, which becomes the ground point in the electrical network at the railway system. One of such autotransformers can be seen in the box labeled as 'AT. Three different levels of the train modeling can be seen in the case. The first level, the closest to the real one, is depicted in a box labeled as 'TR1'. Full switching level power electronics as well as the actual number of propulsion motors were modeled in it. Then, the second way of modeling can be seen in a box labeled as 'TR2'. The train is simplified in terms of the exchange of real power and reactive power (1-phase) between the train and the catenary line is the focus of modeling. Therefore, more complex and realistic description which is available in the first one is omitted. Then, the third level of abbreviation is in the box labeled as 'TR3'. The train is simplified as a load, represented by a simple resistance. The box labeled as 'SP' represents a section post, where one side supply is isolated from the other. If there is a fault on a side, then the circuit breaker in the SP turns on, connecting the other side to the portion of the network which had been supplied by one side before the fault. The box labeled as '87T' models the 87T Scott transformer differential protection element as well as the fault control logic. Lastly, those portions marked by the arrow labels represents the lines in the system. In the simulation case, variable length PI section models were used, in order to describe an important feature of the railway network, the movement of the train (i.e., load). Then, a train schedule was simulated by using the full detail model. The train was scheduled to travel from a station 'A' to another station, station 'B'. The distance between the stations was set to 1500m, which is not unusual in a metro setting. A notch (or master control) was modeled. The notch would control the acceleration and deceleration (braking) of the train. During the travel, the trajectory of the Iop(operating current) and Ires(restrain current) of the protection element was monitored. The following figure, Figure 8, shows the trajectory:

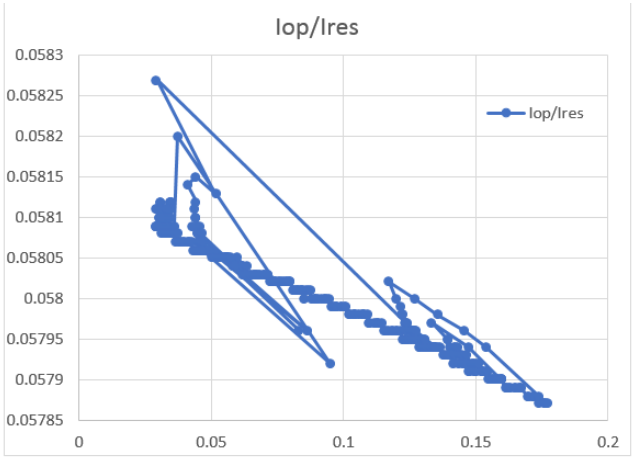

Figure 8 Iop/Ires trajectory

The area where the trajectory exists in the protection curve diagram can be identified in the following figure, Figure 9. Because the area is too small to be easily found, it was marked by an arrow.

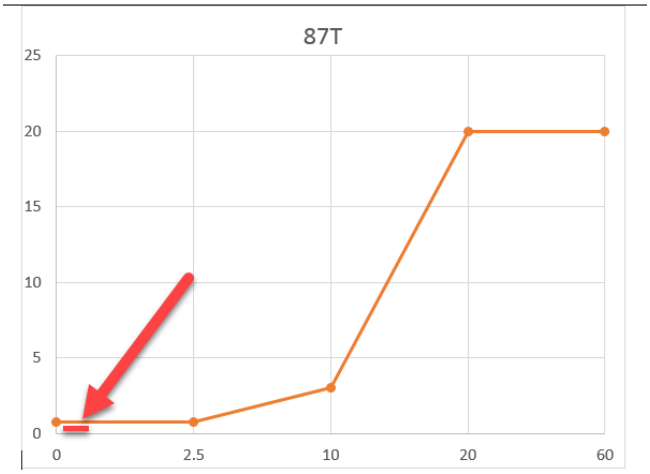

Figure 9 Location of the trajectory

4. Conclusion

A digital twin which represents an electrical railway system was constructed. In order to bring the simulation closer to its real world counterpart, the digital twin was designed as a real time simulation case. It includes the components commonly found in a usual electrified metro system. The proposed digital twin was demonstrated by simulating the behavior of a protection element, 87T Scott

transformer current differential element in various scenarios, in conjunction with the rest of the system. Such digital twin would be expected to find wider applications in the various applications of electrified railway systems.

References

[1] Siemens AG. "On track - Siemens presents the world's first electric railway." https://new.siemens.com/global/en/company/about/history/stories/on-track.html (accessed.

[2] ＪＲ東海. "リニア中央新幹線." https://linear-chuo-shinkansen.jr-central.co.jp/ (accessed.

[3] 나무위키. "츄오신칸센." https://namu.wiki/w/%EC%B8%84%EC%98%A4%20%EC%8B%A0%EC%B9%B8%EC%84%BC (accessed.

[4] R. Kuffel *et al.*, "Expanding an analogue HVDC simulator's modelling capability using a real-time digital simulator (RTDS)," in *ICDS*, College Station, TX, Apr. 1995 1995, pp. 199-204.

[5] H. W. Dommel, "Digital Computer Solution of Electromagnetic Transients in Single- and Multiphase Networks," *IEEE Trans on Power Apparatus and Systems*, vol. PAS-88, no. 4, pp. 388-399, 1969.

[6] K. K. Peter Kuffel, Garth Irwin "The Implementation and Effectiveness of Linear Interpolation Within Digital Simulation," in *IPST '95 - International Conference on Power Systems*, 1995.

[7] H. Jin, "Behavior-mode simulation of power electronic circuits," *Power Electronics, IEEE Transactions on*, vol. 12, no. 3, pp. 443-452, 1997, doi: 10.1109/63.575672.

[8] 황현규, 박희철, and 이은규, "부산도시철도 2 호선 VVVF 인버터 개량 연구," in *한국철도학회 2011 년도 춘계학술대회*, 2011.

[9] 김상훈, *DC 및 AC 모터 제어* Seoul: 복두출판사, 2005.

[10] H. Morimoto, T. Uzuka, A. Horiguchi, and T. Akita, "New type of feeding transformer for AC railway traction system," in *2009 International Conference on Power Electronics and Drive Systems (PEDS)*, 2-5 Nov. 2009 2009, pp. 800-805, doi: 10.1109/PEDS.2009.5385659.

[11] C. Lee, G.-J. Cho, and J. Kim, "Development of Scott Transformer Model in Electromagnetic Transients Programs for Real-Time Simulations," *Applied Sciences*, vol. 11, no. 12, p. 5752, 2021. [Online]. Available: https://www.mdpi.com/2076-3417/11/12/5752.

[12] 김백, *최신전철전력공학*. 기다리, 2015.

[13] 김정철, *전기철도-급전시스템* 기다리, 2002.

In Kwon Park received his bachelor's and master's degree in electrical engineering from Yonsei University, Korea. He received his Ph.D. degree in 2012 from University of Manitoba. His academic advisor was Dr. Ani Gole. Between 1997 and 2002, Dr. Park worked for LG Industrial systems (currently LS Electric), Korea Since 2002, he's been working at RTDS Technologies, Canada. He is a registered professional engineer in the province of Manitoba, Canada.

Sachintha Kariyawasam received the B.Sc. (Eng.) degree in Electrical Engineering from the University of Moratuwa, Sri Lanka, in 2013, and the M.Sc. degree in Electrical Engineering from the University of Manitoba, Canada, in 2016. Currently, he is a Simulation Engineer with RTDS Technologies Inc., Canada. Mr. Kariyawasam is a registered professional engineer in the province of Manitoba, Canada. His research interests include power system protection, renewable energy integration, digital real-time simulations and IEC 61850-based substation automation.

D e a n Ouellette received the diploma in Electrical Engineering Technology from Red River College, Canada, in 1986. Prior to joining RTDS Technologies Inc., Canada in 2004, Mr. Ouellette worked at Manitoba Hydro, BC Hydro, SEL labs, and NXT Phase. Currently, he is the manager of Protection and Automation with RTDS. Mr. Ouellette is a senior member of IEEE, member of IEEE/PSRC, member of IEC TC57/WG10, and vice-chair for the Canadian National Committee to IEC TC57. His research interests include power system protection, PMUs, digital real-time simulations and IEC 61850-based substation automation.

Yi Zhang (M'05-SM'11-F'19) joined RTDS Technologies, Inc., Winnipeg, in 2000 and currently holds the position of the vice president R&D and CTO. Dr. Zhang also serves as an adjunct professor at the University of Manitoba and an editor for IEEE Transactions on Power Delivery. He is a registered professional engineer in the province of Manitoba, Canada.

Joorak Kim was born in South Korea in 1974. He received the B.S., M.S., and Ph.D. degrees in electrical engineering from Hongik University, Seoul, South Korea, in 1997, 1999, and 2010, respectively. He is currently a Principal Researcher with Korea Railroad Research Institute, Uiwang, South Korea. His research interests include static and dynamic analysis of traction power supply system.

Gyu-Jung Cho (S'14) was born in South Korea, in 1986. He received the B.S., M.S. and Ph.D. degrees, in 2012, 2014 and 2019, respectively, from the College of Electrical and Computer Engineering, Sungkyunkwan University, Suwon, South Korea. He is currently a Senior Researcher with the Smart Electrical & Signaling Division, Korea Railroad Research Institute, Uiwang, South Korea. His research interests include power system dynamics, electric railway system operation and protection, integration of renewable energy resources, and distribution system planning.